

Synthesis and Characterization of a Novel Symmetrical Sulfone-Substituted Polyphenylene Vinylene (SO₂EH-PPV) for Applications in Light Emitting Devices

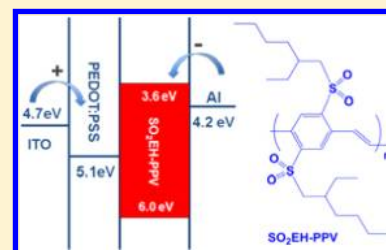
Emir Hubijar,[†] Alexios Papadimitratos,^{||} Doyun Lee,[†] Anvar Zakhidov,^{‡,§} and John P. Ferraris^{*,†,§}

[†]Department of Chemistry, [‡]Department of Physics, and [§]The Alan G. MacDiarmid Nanotech Institute, The University of Texas at Dallas, 800 West Campbell Rd, Richardson, Texas 75080-3021, United States

^{||}Solarno Inc., 153 Hollywood Drive, Coppell, Texas 75019, United States

S Supporting Information

ABSTRACT: A novel symmetrical alkylsulfonyl-substituted poly(phenylenevinylene) derivative, poly [2,5-bis-(2'-ethylhexylsulfonyl)-1,4-phenylene]vinylene (SO₂EH-PPV), was synthesized via palladium-catalyzed Stille coupling, and its electronic and optical properties were investigated. The novel PPV derivative was characterized by NMR, UV-visible absorption, photoluminescence, gel permeation chromatography, infrared spectroscopy, and cyclic voltammetry (CV). The polymer with M_w of 27 800 and a polydispersity index of 2.6 is readily soluble in common organic solvents, such as THF, chloroform, and toluene. The fluorescence quantum yield of the polymer, determined against rhodamine 6G in dilute aqueous solutions, was 0.95. The HOMO and LUMO levels of SO₂EH-PPV were calculated to be -6.0 and -3.61 eV, respectively. The results obtained by CV suggest that SO₂EH-PPV is a strong electron acceptor polymer. Single layer stable polymer light-emitting diode devices with the configuration of (ITO/PEDOT:PSS/SO₂EH-PPV polymer/Al) were fabricated exhibiting a green light emission.



INTRODUCTION

Conjugated polymers are a novel class of semiconductors that have been intensively studied as electroluminescent materials for application in polymer light-emitting diodes (PLEDs).^{1–6} They offer the advantages of low cost and easy processing, which make them potential replacements for expensive inorganic counterparts.^{7,8} Among the organic conjugated polymers, poly(*p*-phenylenevinylene)s (PPVs) have received considerable attention for application in PLEDs after the first report by Burroughes et al. in 1990.⁹ PPV polymers have good chemical and mechanical properties, high hole mobilities, and require relatively low driving voltages in optoelectronic devices making them a suitable material in PLEDs.^{10–12} The performance of the PLED devices using conjugated polymers can be limited due to large mobility mismatch between holes and electrons, leading to a recombination zone very close to one of the electrodes where traps and defects are likely to be prevalent.^{1,13,14} Since hole mobility is often larger than electron mobility in conjugated polymers, the recombination zone is likely to occur close to the cathode.¹⁵ Apart from the polymer's charge transport properties, the operation of a PLED device relies greatly upon injection of charges from the corresponding electrodes. Hence, charge injection efficiency depends upon the suitable selection of electrode materials as well.¹ Therefore, the size of the energy barrier between the work function of the electrode and the energy level of the HOMO (for the anode) or LUMO (for the cathode) level of the polymer must be minimal for efficient charge injection.^{16,17} Because balanced charge injection is required, the energy barriers should be of

comparable sizes.^{1,18} Due to these limitations, different acceptor-types of polymers, including cyano-substituted alkoxy-substituted PPVs (poly[(2-(2'-ethylhexyloxy)-5-methoxy)-1,4-phenylene-(1-cyanovinylene)]) (MEH-CN-PPV) have been extensively investigated and showed great improvements in electroluminescence (EL) efficiency due to their high electron affinity.^{16,19–25} The cyano (electron-withdrawing) substituent on the vinylene linkage in the backbone of the polymer serves to lower both the LUMO and HOMO energy levels.^{26,27} Lowering the LUMO energy level enhances the electron injection which then allows for an effective recombination of electrons and holes resulting in a higher device performance. Sulfone moieties are also widely known for their electron withdrawing properties (comparable to cyano) and can be directly attached to the polymer's backbone to afford electron acceptor materials.^{28–31}

The attractive combination of excellent optical and electronic properties of the conjugated PPVs has encouraged our synthesis of a novel symmetrical alkylsulfonyl-substituted poly(phenylenevinylene) derivative, poly[2,5-bis-(2'-ethylhexylsulfonyl)-1,4 phenylene]vinylene (SO₂EH-PPV) utilizing the Stille-coupling reaction. In this paper, we report detailed synthesis and characterization of this novel polymer and

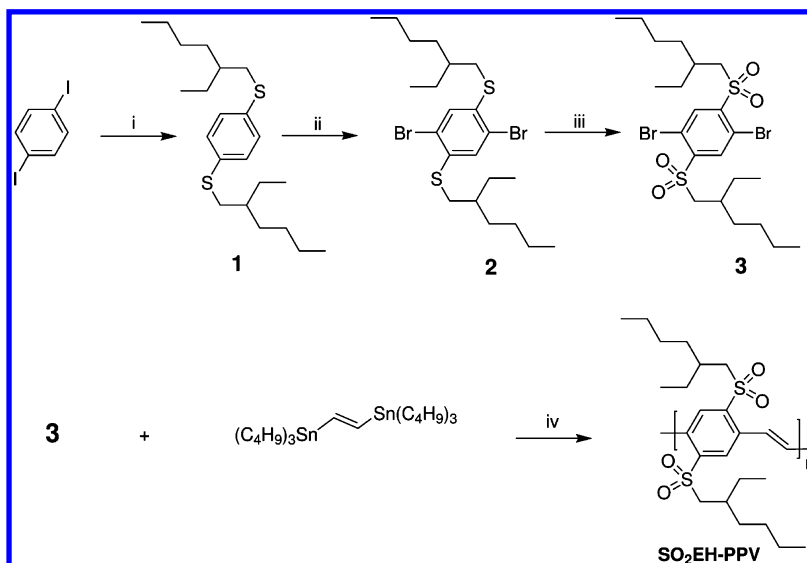
Special Issue: Paul F. Barbara Memorial Issue

Received: August 14, 2012

Revised: November 19, 2012

Published: November 20, 2012

Scheme 1. Synthetic Routes to Precursor Monomers and Polymer



Reagents and conditions: (i) 20 mol % CuI, neocuproine, 4 equiv. K₃PO₄, DMF, 2-ethylhexanethiol, 115 °C, 48 h; (ii) Br₂, I₂, CH₂Cl₂, 3 d at room temp; (iii) H₂O₂, AcOH, 3 h reflux; (iv) *trans*-1,2-bis (tri-*n*-butylstannyl) ethylene, toluene, Pd(PPh₃)₄, 120 °C, 24 h.

preliminary results using this electroluminescent material in light emitting diodes.

EXPERIMENTAL SECTION

Materials. All chemicals, unless otherwise stated, were obtained from Sigma Aldrich Chemical Co. and were used as received. All solvents were distilled over appropriate drying agent(s) prior to use and were purged with nitrogen. Water content (<20 ppm) was determined with a Karl Fischer titrator (Denver Instruments, model 270).

Characterization. UV–visible absorption spectra were collected using a Shimadzu UV-1601PC UV–visible spectrophotometer controlled by UV-1601PC software. Emission spectra were collected using a Jobin-Yvon fluorimeter controlled by Datamax software version 1.03. FT-IR spectra were collected using a Nicolet/Avatar 360 FT-IR controlled by EZ-OMNIC software. The fluorescence quantum yield in chloroform solution was determined relative to a Rhodamine 6G standard in dilute aqueous solution. Corrections for refractive indices and differences in optical densities were applied. Molecular weights were obtained via gel permeation chromatography (GPC) on two series-connected ViscoGel I-Series (I-MBHMW-3078) columns with a Viscotek triple array detector 302 (TDA 302: refractometer, light scattering, and viscometer) using THF eluent at 1 mL/min flow rate. Polystyrene standards were used for calibration. Data were analyzed using Viscotek OmniSEC software, version 3.0. High resolution mass spectra (HRMS) were recorded on a mass spectrometer operating in positive ESI(+) mode. ¹HNMR and ¹³CNMR spectra were obtained at room temperature using a JEOL FX-270 MHz spectrometer using TMS as an internal standard. TGA thermograms were obtained using a Perkin-Elmer PYRIS 1 thermogravimetric analyzer heated from 60 to 800 °C at 10 °C/min. Cyclic voltammograms (CV) were obtained using a standard three-electrode cell connected to an EG&G Princeton Applied Research potentiostat/galvanostat 273A with PowerSuite software. All CV measurements were done inside a nitrogen-filled glovebox. Chloroform solutions of the PPVs were drop cast onto platinum electrodes and the

resulting films were dried in vacuum at 50 °C for 2 h. A solution of tetrabutylammonium hexafluorophosphate (TBAPF₆) in dry acetonitrile (0.1 M) was used as the electrolyte, and the reference electrode was Ag/Ag⁺ (0.01 M AgNO₃ in TBAPF₆/dry acetonitrile). The counter electrode was a platinum wire. CV measurements of the SO₂EH-PPV homopolymer were scanned at constant scan rate of 50 mV/s. TMAFM (tapping mode atomic force microscopy) studies were carried out on a VEECO-dimension 5000 scanning probe microscope with a hybrid xyz head equipped with Nano-Scope Software. AFM images were obtained using silicon cantilevers with nominal spring constant of 42 N/m and nominal resonance frequency of 300 kHz (OTESPa). Nanoscope 7.30 software was used for surface imaging and image analysis. All AFM measurements were conducted under ambient conditions. Cantilever oscillation amplitude was equal to ca. 380 mV, and all images were acquired at 1 Hz scan frequency. Sample scan area was 1 μm. The AFM images were obtained on the actual PLED devices. Samples were prepared from chloroform (10 mg/mL) via spin-casting. Light emitting devices were fabricated using glass/indium tin oxide substrates. The glass substrates were high quality display glass (Corning 1737) with very low surface roughness. The sheet resistance of the indium tin oxide (ITO) layer was about 10 Ω/□, with a film thickness of 120 nm and an optical transparency of 85%. The hole injection layers, PEDOT:PSS (CLEVIOS PVP CH 8000), were spun cast at 5000 rpm, and the layer thickness was 70 nm on average. SO₂EH-PPV solutions in chloroform were prepared at a concentration of 10 mg/mL. The polymeric solutions were spun cast at 2000 rpm onto the glass/ITO/PEDOT:PSS substrates with average film thicknesses of 100 nm according to profilometry measurements (Ambios Technology, XP-1). An interface modification thin layer of cesium carbonate (Cs₂CO₃) was spun cast before cathode fabrication to improve electron injection. The cesium carbonate was dissolved in 2-ethoxyethanol at 0.2 wt %. The patterned aluminum (Al) cathode was deposited using thermal evaporation through a shadow mask. All device characterizations were done using a Keithly 236 source measurement unit and a Photo Research

PR-650 Spectrocolorimeter that provided the current density–voltage (J – V) and luminance–voltage (L – V).

Monomer Synthesis. Monomer 1 (1,4-dibromo-2,5-bis(2-ethylhexylsulfonyl)benzene), monomer 2 (1,4-bis(2-ethylhexylsulfonyl)-2,5-diethylthio)benzene), and all intermediates were synthesized according to the reported literature with modifications. The synthetic pathways to all monomers are displayed in Scheme 1.

1,4-Bis-(2-ethylhexylthio)benzene (1). 1,4-Diiodobenzene (5 g, 15.2 mmol), copper iodide (0.58 g, 21 mol %), neocuproine (0.63 g, 20 mol %), and potassium phosphate tribasic (13.0 g, 4.1 equiv) were placed in a 250 mL RB-flask while maintaining a nitrogen flow. DMF (100 mL, anhydrous) was injected, and the reaction assumed a clear, deep red color. 2-Ethylhexanethiol (5.8 mL, 2.2 equiv) was injected into the reaction, and the color turned orange. The reaction mixture was heated to 110 °C where-upon the reaction turned to a white turbid color and was left to stir overnight under nitrogen. TLC on silica analysis (hexanes) after 48 h of reaction time showed disubstituted product without the presence of the monosubstituted side product. The reaction mixture was left to cool to room temperature and ethyl acetate (30 mL) was added and then filtered. The organic layer was collected, washed with deionized water, 7.5% sodium bicarbonate solution, and brine (2 × 100 mL), and dried over sodium sulfate. The solvent was removed under reduced pressure affording a deep purple colored oil. The oil was purified through chromatography on a silica gel packed column, using hexanes as the eluent to afford 4.45 g (80%) of clear colorless oil. ^1H NMR (CDCl_3 , 270 MHz): δ 7.24–7.23 (s, 4H, $\text{C}^{\text{ar}}\text{-H}$), 2.87–2.85 (d, 4H, S-CH_2), 1.60–1.26 (m, 18H, other CH_2), 0.92–0.86 (t, 12H, CH_3). ^{13}C NMR (CDCl_3 , 270 MHz): δ 135.0 (s, $\text{C}^{\text{ar}}\text{-S}$), 129.7 (s, $\text{C}^{\text{ar}}\text{-C}$), 39.1 (s, S-CH_2), 38.5 (s, CH), 32.4, 25.7, 23.1 (s, CH_2), 14.2 (s, CH_3), 10.8 (s, other CH_3).

2,5-Dibromo-1,4-bis(2-ethylhexylthio)benzene (2). A catalytic amount of iodine (0.066 g) was added to a solution of 3 g of 1,4-bis-(2'-ethylhexylthio)benzene (1) (8.18 mmol) in CH_2Cl_2 (30 mL) maintained at 0 °C. With constant stirring in the dark, bromine (1.048 mL 20.5 mmol) was added to the solution which was then stirred at room temperature for 3 days. The reaction was terminated by adding 10% aqueous solution of sodium sulfite Na_2SO_3 and then the mixture was extracted with chloroform. The organic phase was collected and washed three times with water and dried over sodium sulfate. The solvent was removed under reduced pressure to afford a yellow oil. The oil was purified through a silica gel packed column, using hexanes as the eluent to yield 2.9 g (68% yield) of a clear colorless oil. ^1H NMR (CDCl_3 , 270 MHz): δ 7.36 (s, 2H, $\text{C}^{\text{ar}}\text{-H}$), 2.87–2.85 (d, 4H, S-CH_2), 1.69–1.28 (m, 18H, other CH_2), 0.92–0.86 (t, 12H, CH_3). ^{13}C NMR (CDCl_3 , 270 MHz): δ 137.0 (s, $\text{C}^{\text{ar}}\text{-S}$), 131.8 (s, $\text{C}^{\text{ar}}\text{-H}$), 123.4 ($\text{C}^{\text{ar}}\text{-Br}$), 39.1 (s, S-CH_2), 38.5 (s, CH), 33.1, 28.9, 25.4, 23.8 (s, CH_2), 14.2 (s, CH_3), 10.8 (s, other CH_3).

1,4-Dibromo-2,5-bis(2-ethylhexylsulfonyl)benzene (3). To a solution of 2 g (3.81 mmol) of 2,5-dibromo-1,4-bis-(2'-ethylhexylthio)benzene in 14 mL of warm glacial acetic acid was added 8 mL of 35% hydrogen peroxide in 7.2 mL of glacial acetic acid. When the initial reaction had subsided, another 8 mL of the 35% hydrogen peroxide was added, and the solution was refluxed for 3 h at 120 °C. The crystalline white solid was obtained when the mixture was poured into water. Mp. 104–106 °C. FTIR (KBr pellet: cm^{-1}): 2852, 2924 (aliphatic C–H), 1149, 1350 ($-\text{SO}_2$). ^1H NMR (CDCl_3 , 270 MHz): δ 8.49 (s,

2H, $\text{C}^{\text{ar}}\text{-H}$), 3.39–3.34 (dd, 4H, $\text{SO}_2\text{-CH}_2$), 1.97–2.096 (septet, 2H, CH), 1.65–1.21 (m, 16H, other CH_2), 0.92–0.86 (t, 12H, CH_3). ^{13}C NMR (CDCl_3 , 270 MHz): δ 144.7 (s, $\text{C}^{\text{ar}}\text{-SO}_2$), 138.1 (s, $\text{C}^{\text{ar}}\text{-H}$), 120.5 ($\text{C}^{\text{ar}}\text{-Br}$), 57.4 (s, $\text{SO}_2\text{-CH}_2$), 34.4 (s, CH), 32.4, 28.2, 25.9, 22.7 (s, CH_2), 14.1 (s, CH_3), 10.2 (s, other CH_3). HRMS (ESI+) calculated for $\text{C}_{22}\text{H}_{36}\text{Br}_2\text{O}_4\text{S}_2$: 609.0314 ($\text{M}+\text{Na}^+$). Found: 609.0325 ($\text{M}+\text{Na}^+$).

PPV Polymer Synthesis. Polymerization was carried out via Stille coupling between monomer 3 and *trans*-1,2-bis(tri-*n*-butylstannyl)ethylene following the reported literature with modifications. The synthetic pathway is displayed in Scheme 1.

Poly[2,5-bis(2-ethylhexylsulfonyl)-1,4-phenylene-vinylene]. To a 3-neck 50 mL flask were added 0.11 g (0.17 mmol) of *trans*-1,2-bis(tri-*n*-butylstannyl)ethylene and 0.1 g (0.17 mmol) of 1,4-dibromo-2,5-bis(2-ethylhexylsulfonyl)benzene. Then, 6 mL of dry toluene were added under the protection of nitrogen. The solution was flushed with nitrogen for 10 min, and then 0.004 g (1% molar) of Pd (PPh_3)₄ dissolved in 2 mL of toluene was added to the reaction mixture. After another flushing with nitrogen for 20 min, the reaction was heated at reflux (120 °C) for 48 h. After cooling to room temperature, the polymerization mixture was poured into 300 mL of methanol. The precipitated polymer was collected by filtration using a Millipore Durapore 0.45 μm membrane filter. The collected polymer was then subjected to Soxhlet extraction with methanol, hexane, and chloroform. The polymer was then dried under vacuum overnight at 50 °C. FTIR (KBr pellet: cm^{-1}): 2859, 2929 (aliphatic C–H), 1151, 1351 ($-\text{SO}_2$). ^1H NMR (CDCl_3 , 270 MHz): δ 8.31 (s, 2H, $\text{C}^{\text{ar}}\text{-H}$), 3.6–3.3 (dd, 4H, $\text{SO}_2\text{-CH}_2$), 2.1–1.8 (septet, 2H, CH) 1.65–1.21 (m, 16H, other CH_2), 0.92–0.86 (t, 12H, CH_3). GPC (THF): $M_n = 10\,600$, $M_w = 27\,800$, polydispersity index = 2.6. UV–vis (solution 10^{-5} M in CHCl_3): $\lambda_{\text{abs,max}}/\text{nm} = 442$, (as film): 444. PL (solution 10^{-5} M in CHCl_3): $\lambda_{\text{em,max}}/\text{nm} = 505$, 534 (as film): 548. TGA_T: 250 °C (onset, 5% weight loss). Cyclic voltammetry (HOMO/LUMO = -6.0 eV/ -3.61 eV).

RESULTS AND DISCUSSION

Synthesis and Characterization of Polymer. Synthetic steps toward monomers and a $\text{SO}_2\text{EH-PPV}$ polymer are outlined in Scheme 1. In the first step, S-alkylation was completed using a modified synthetic pathway based on the Ullman-type copper(I)-catalyzed cross-coupling reaction of aryl halides with alkanethiols.^{32–34} Once S-alkylation was completed, the final monomer was obtained via direct bromination of the 1,4-bis-(2'-ethylhexylthio)benzene at the para sites, followed by oxidation of sulfur to sulfone (Scheme 1).^{30,35–37} The synthesis of the $\text{SO}_2\text{EH-PPV}$ was carried out by palladium-catalyzed Stille coupling reaction utilizing the monomer 3 and commercially available *trans*-1,2-bis(tri-*n*-butylstannyl)ethylene.^{26,38} The polymer obtained with a M_w of 27 800 and a polydispersity index (PDI) of 2.6 was readily soluble in common organic solvents, such as THF, chloroform and toluene. The good solubility can be attributed to the two sulfone-alkyl side chains attached to phenyl ring. All of the polymerization data are summarized in Table 1. The polymer forms smooth and uniform films on glass substrates when cast from chloroform solutions, which can be an advantage for their potential applications as active layers in electronic devices. The chemical structures of all of the monomers and the polymer were verified with NMR and FTIR analyses. In the ^1H NMR spectrum in Figure S1, the signals at around δ 7.5–8.6 ppm are

Table 1. Polymerization Data for the Conjugated Polymer

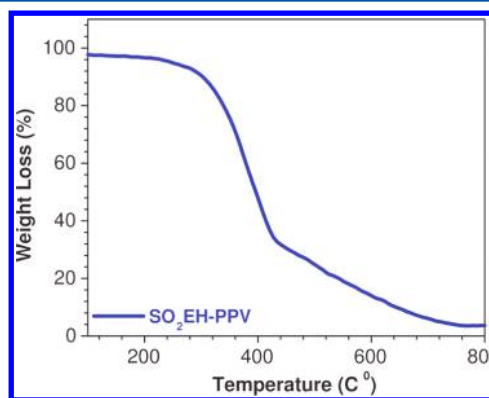
polymer	M_n^a	M_w^a	PDI ^a	yield (%)	T_d (°C) ^b
SO ₂ EH-PPV	10 600	27 800	2.61	64	250

^aDetermined using GPC (eluent: THF; polystyrene standards).

^bTemperature at 5% weight loss by a heating rate of 10 °C/min under nitrogen.

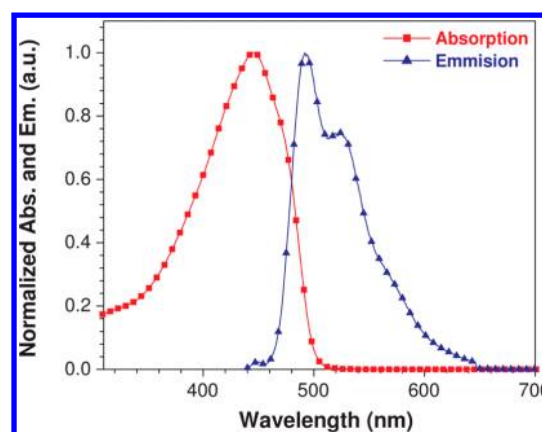
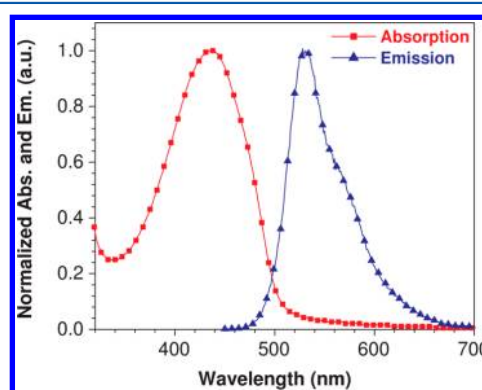
assigned to the aromatic and conjugated vinylene protons which are shifted downfield due to the electron-withdrawing nature of sulfone units. Moreover, the methine proton signal can be seen at 2.6 ppm as a broadened peak as opposed to a septet previously observed in monomers 3 and is shifted downfield. ¹H NMR spectrum also shows the characteristic peak of the methylene protons adjacent to the sulfone at 3.1–3.3 ppm. Finally, a cluster of broadened peaks between 0.2 and 1.9 ppm correspond to the rest of the proton signals from the side alkyl chains. The chemical structure of the SO₂EH-PPV polymer is also reflected in the FTIR spectra, which are shown in Figure S2. The vinylic carbon–carbon double bond stretch was observed at 1015 and 1032 cm⁻¹. The absorption bands at 1151 and 1351 cm⁻¹ correspond to sulfonyl groups, and the signal observed from 3000 to 2800 cm⁻¹ is attributed to C–H stretch from the aliphatic chains.

Thermal Properties. The thermal properties of the resulting polymer were investigated by thermogravimetric analysis (TGA) at a heating rate of 10 °C/min under nitrogen flow (Figure 1). The polymer exhibited good thermal stability

**Figure 1.** Thermogravimetric analysis of the SO₂EH-PPV polymer under N₂.

with a 5% weight loss onset occurring at 250 °C with significant weight losses at 380 °C (30% loss) and 410 °C (50% loss). The thermal stability of SO₂EH-PPV is adequate for use in LED or other electronic applications.

Optical Properties. The optical properties of the novel polymer were investigated by measuring UV–visible absorption and photoluminescence (PL) spectra in both dilute chloroform solutions and as thin films. UV–visible absorption and PL spectra in solution and as thin films are shown in Figures 2 and 3, respectively, and are summarized in Table 2. The absorption and emission maxima in dilute solutions appear at 442 and 505 nm (with a shoulder signal at 534 nm), respectively. Figure 3 shows that spun cast film of the polymer has a red-shifted emission maxima compared to its corresponding solution spectra. The polymer in the solid state emits an intense green light upon excitation. The absorption and emission maxima of thin films are 444 and 548 nm, respectively. The optical band

**Figure 2.** Normalized UV–visible absorption and photoluminescence of SO₂EH-PPV polymer in solution (10⁻⁵ M in CHCl₃).**Figure 3.** Normalized solid-state UV–visible absorption and photoluminescence of SO₂EH-PPV polymer (film cast from 10 mg/mL in CHCl₃ solutions).**Table 2.** Optical Properties of the Polymer SO₂EH-PPV

polymer	$\lambda_{\text{abs.max}}$ (nm, UV–vis)		$\lambda_{\text{em.max}}$ (nm, PL)		Φ^c
	solution ^a	film ^b	solution ^a	film ^b	
SO ₂ EH-PPV	442	444	505, 534	548	0.95

^a1 × 10⁻⁵ M in CHCl₃. ^bSpin-coated from a 10 mg/mL solution.

^cQuantum yield of the polymer solution using Rhodamine 6G ($\Phi = 0.95$) as a standard.

gap for the polymer SO₂EH-PPV, estimated from the absorption spectra's onset in a solid state, is 2.39 eV (Table 3). The fluorescence quantum yield of the polymer, determined against rhodamine 6G in dilute aqueous solutions, is 0.95.

Morphology. The morphology of the polymer SO₂EH-PPV in PLED devices was investigated using TMAFM microscopy. Films were deposited by spin-casting from chloroform solutions with a concentration of 10 mg/mL followed by annealing at 120 °C for 5 min. As can be seen from the AFM topography images in Figure 4, the film from the resulting SO₂EH-PPV/chloroform solution has a smooth surface. The rms roughness values were obtained by completing roughness analysis of the surface which revealed that the average root-mean-square roughness (R_{rms}) over 2 $\mu\text{m} \times 2 \mu\text{m}$ is below 3 nm.

Electrochemical Properties. Cyclic voltammetry (CV) was performed to investigate electrochemical behavior and to estimate electronic energy levels (HOMO and LUMO levels) of the SO₂EH-PPV polymer. Figure 5 shows the CV of the homopolymer using TBAPF₆ as supporting electrolyte in

Table 3. Electrochemical Properties of the Polymer SO₂EH-PPV

polymer	$\lambda_{\text{abs.max}}$ (nm, film)	λ_{onset} (nm)	$E_{\text{opt.gap}}$	$E_{\text{onset.ox}}$ (V)/HOMO ^b (eV)	$E_{\text{onset.red}}$ (V)/LUMO ^c (eV)
SO ₂ EH-PPV	444	518	2.39 ^a	1.3/−6.0	−1.10/−3.61

^aEstimated from the onset wavelength of optical absorption. ^bHOMO was calculated from the LUMO level and optical band gap. ^cLUMO was calculated from the onset reduction potential.

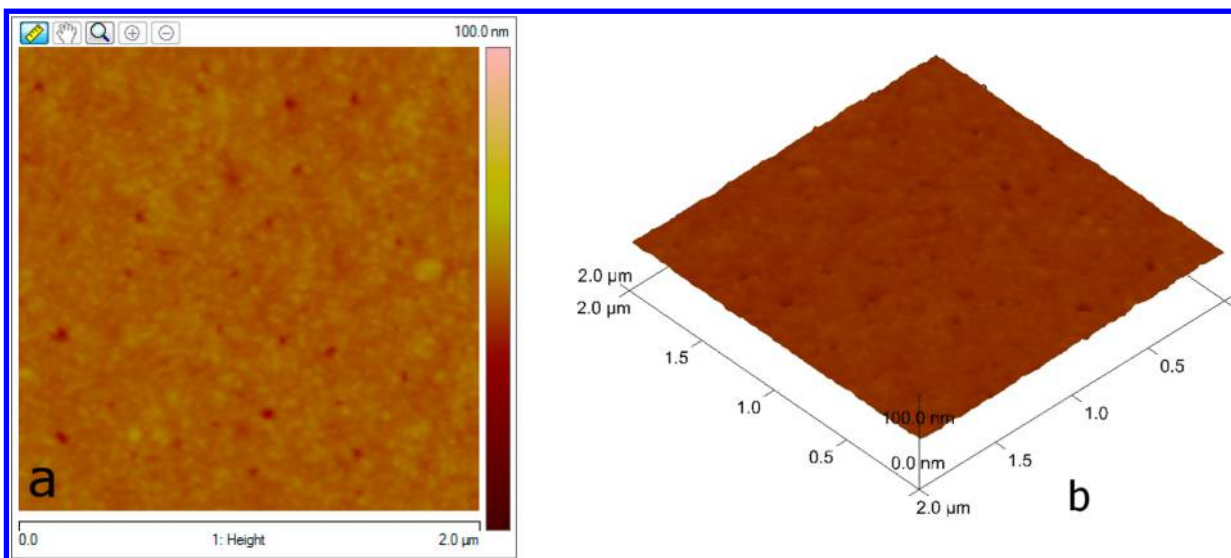


Figure 4. TMAFM height image of the SO₂EH-PPV based PLED devices spin cast from the chloroform solutions (10 mg/mL); (b) 3D height TMAFM image of the SO₂EH-PPV based PLED devices deposited by spin-casting from chloroform solution (10 mg/mL). Scan size: 2 μm \times 2 μm .

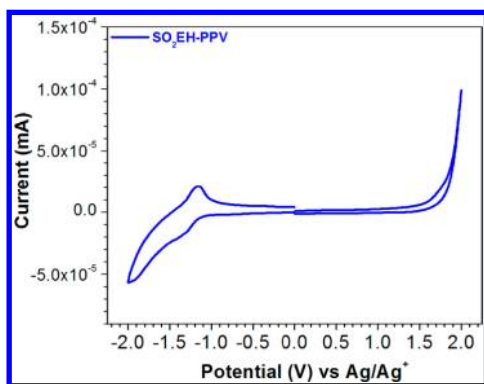


Figure 5. Cyclic voltammogram of SO₂EH-PPV.

acetonitrile solution with platinum working electrodes, a platinum wire counter electrode and an Ag/AgNO₃ reference electrode under the N₂ atmosphere. The ionization potential (HOMO level) and electron affinity (LUMO level) of the SO₂EH-PPV polymer were calculated from the onset potentials of oxidation and reduction relative to the vacuum. Hence, the HOMO and LUMO levels as well as the energy band gap ($E_{\text{g.ec}}$) could be computed according to the following equations:

$$\text{HOMO} = -e(E_{\text{onset}}^{\text{ox}} + 4.71) \text{ (eV)} \quad (1)$$

$$\text{LUMO} = -e(E_{\text{onset}}^{\text{red}} + 4.71) \text{ (eV)} \quad (2)$$

$$E_{\text{g.ec}} = E_{\text{onset}}^{\text{ox}} - E_{\text{onset}}^{\text{red}} \text{ (eV)} \quad (3)$$

where $E_{\text{onset}}^{\text{ox}}$ and $E_{\text{onset}}^{\text{red}}$ are the measured potentials relative to Ag/Ag⁺. Detailed electrochemical properties as well as the energy level parameters of the PPV homopolymer are listed in Table 3. The cyclic voltammogram of SO₂EH-PPV displays a distinct reversible n-doping/dedoping process (reduction/

reoxidation). Figure 5 shows the onset reduction potential of SO₂EH-PPV of −1.10 V vs Ag/Ag⁺, which corresponds to the lowest unoccupied molecular orbital (LUMO) energy level of −3.61 eV according to eq 2. Ionization potential value of −6.0 eV (HOMO level) was calculated by utilizing the onset oxidation potential (1.3 V vs Ag/Ag⁺) into the eq 1. Compared with the n-doping/dedoping process, the cyclic voltammogram of the SO₂EH-PPV polymer showed an irreversible oxidation peak. The optical band gap for the resulting polymer, calculated from the onset of absorption, was 2.39 eV, which is in a good agreement with the electrochemical band gap of 2.4 estimated from the reduction (−1.1 eV) and oxidation (1.3 eV) onset as seen in Figure 5. Cyclic voltammetry suggests that SO₂EH-PPV is a strong electron-acceptor and could be an attractive material for other applications in electronic devices.

Electroluminescent Properties. PLED devices based on the SO₂EH-PPV polymer were fabricated with the following device configurations: glass/ITO/PEDOT:PSS/SO₂EH-PPV/Al and glass/ITO/PEDOT:PSS/SO₂EH-PPV/CsCO₃/Al. Indium tin oxide (ITO) with a sheet resistance of 10 Ω / \square was used as an anode. An aluminum (Al) cathode was deposited onto the device using thermal evaporation. The Fermi levels of ITO and Al were approximately −4.7 and −4.2 eV, respectively.^{1,15} The hole transporting layer composed of poly(3,4-ethylene dioxythiophene):polystyrene sulfonate, PEDOT:PSS with a work function of 5.1 eV,^{39,40} was spun cast as a thin layer of approximately 70 nm onto the ITO/glass substrate. The active/emissive layer was prepared via spin coating of the polymer solution in chloroform (10 mg/mL) on top of the ITO/PEDOT:PSS covered ITO anode, and was annealed at 120 $^{\circ}\text{C}$ for 5 min. The thickness of the emissive layer was approximately 100 nm for both configurations. The current density–voltage (J – V) and luminescence–voltage (L – V) characteristics of glass/ITO/PEDOT:PSS/SO₂EH-PPV/Al

and glass/ITO/PEDOT:PSS/SO₂EH-PPV/Cs₂CO₃/Al devices are shown in Figure 6. The color of EL spectra is typically

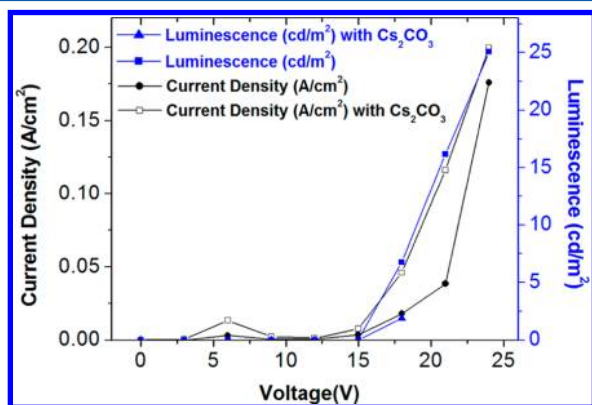


Figure 6. Current density–voltage (J – V) and luminescence–voltage (L – V) curves of devices: (a) glass:ITO/PEDOT:PSS/polymer (SO₂EH-PPV)/Al and (b) glass:ITO/PEDOT:PSS/polymer (SO₂EH-PPV)/Cs₂CO₃/Al.

defined by their CIE (Commission Internationale de L'Eclairage) chromaticity coordinates (x , y).^{41,42} The CIE coordinates for the EL spectra of SO₂EH-PPV are 0.36 and 0.55. Both device configurations based on SO₂EH-PPV polymer showed uniform and stable green emission. The EL spectrum of the polymer is almost identical to the PL (see Figure 7) indicating that the recombination zone in EL and the

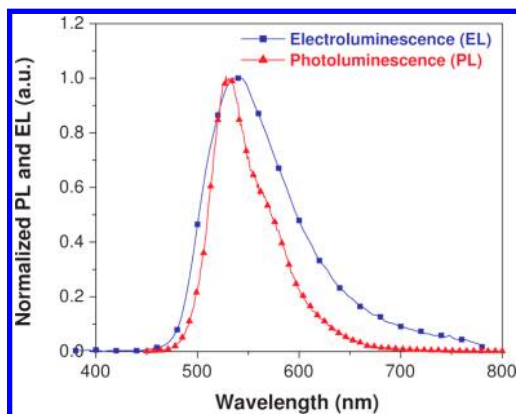


Figure 7. PL and EL spectra of devices glass:ITO/PEDOT:PSS/polymer (SO₂EH-PPV)/Al.

emission mechanism in PL originated from the same excited state. The poor efficiency of the fabricated devices is expected because of a large mismatch of a HOMO level of SO₂EH-PPV and the ITO anode work function (see Figure 8). Therefore, a large hole injection barrier is formed at the interface of the anode and the active layer affecting the efficiency of the PLED devices. The best performance was obtained with the ITO/PEDOT:PSS/SO₂EH-PPV/Al devices, whereas the fabricated devices with the additional electron injection layer of Cs₂CO₃ had lower luminance. Figure 6 shows that the devices with Cs₂CO₃ are operating at higher current density, indicating improved electron injection from the cathode to the active/emissive layer (SO₂EH-PPV). However, the performance of PLED devices suffered by utilizing an electron injection layer (Cs₂CO₃) due to unbalanced ratio of positive and negative charges during operation of the PLEDs. The schematic

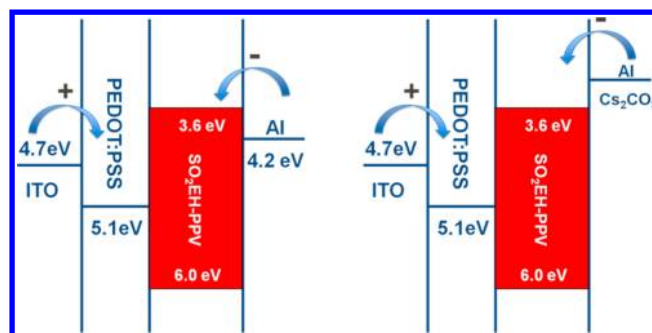


Figure 8. Schematic diagram of the PLED device configurations and illustration of SO₂EH-PPV's HOMO and LUMO levels.

diagrams in Figure 8 show two different types of devices where the thin Cs₂CO₃ layer decreases the effective work function of the cathode to 2.2 eV by forming Al–O–Cs complex^{43,44} and eliminates the electron injection barrier between the Al and LUMO level of SO₂EH-PPV. As evidenced by the obtained results, the more evenly matched injection of carriers from both electrodes yields a more balance charge ratio and hence better efficiency in PLED devices. In this particular polymer, the sulfone substituent (electron withdrawing) which is directly attached to the PPV benzene ring has a large influence on lowering both LUMO and HOMO levels of the polymer and consequently contributes to the poor efficiency of the constructed LED devices. In order to mitigate these limitations and take advantage of the excellent intrinsic properties of SO₂EH-PPV, we are currently optimizing/designing new LED device configurations to better match the HOMO and LUMO levels of the polymer with the anode and cathode. This would potentially improve the injection of holes and electrons, and overall efficiency of the device.

CONCLUSION

In this paper, we have successfully synthesized a novel symmetrical sulfone-substituted polyphenylene vinylene (PPV) polymer (SO₂EH-PPV) via Stille-coupling reaction. The polymer with M_w of 27 800 and a polydispersity index (PDI) of 2.6 is readily soluble in common organic solvents, such as THF, chloroform, and toluene. In addition, it exhibits a good thermal stability with 5% weight loss onset occurring at 250 °C. The optical band gap for the resulting polymer, calculated from the absorption spectra's onset in a solid state, was 2.39 eV. The fluorescence quantum yield of the polymer, determined against a rhodamine 6G standard in dilute aqueous solution, was 0.95. Stable PLED devices based on SO₂EH-PPV polymer were fabricated but exhibited low efficiencies due to the deep HOMO level of the SO₂EH-PPV and its mismatch with the work function of the ITO anode. The cyclic voltammogram of SO₂EH-PPV displays a distinct reversible n-doping/n-dedoping process, with the onset reduction potential at -1.1 V vs Ag/Ag⁺. Using this potential, the LUMO level of the polymer was calculated to be -3.61 eV. Due to the small current associated with the p-doping in the oxidation process, the HOMO level was calculated (-6.0 eV) from the polymer's optical energy gap and its experimentally determined LUMO level. Cyclic voltammetry suggests that SO₂EH-PPV is a strong electron acceptor conjugated polymer that can be an attractive material for applications in photovoltaic devices as an electron acceptor.

■ ASSOCIATED CONTENT

● Supporting Information

NMR, IR, and quantum yield data are included. This material is available free of charge via the Internet at <http://pubs.acs.org>.

■ AUTHOR INFORMATION

Notes

The authors declare no competing financial interest.

■ ACKNOWLEDGMENTS

Financial support from the Robert A. Welch Foundation (Grant AT-1617) and the U.S. Department of Energy (Grant DE-SC0003664) is gratefully acknowledged.

■ REFERENCES

- (1) Grimsdale, A. C.; Leok Chan, K.; Martin, R. E.; Jokisz, P. G.; Holmes, A. B. *Chem. Rev.* **2009**, *109*, 897–1091.
- (2) Li, Y.; Cao, Y.; Gao, J.; Wang, D.; Yu, G.; Heeger, A. J. *Synth. Met.* **1999**, *99*, 243–248.
- (3) Kraft, A.; Grimsdale, A. C.; Holmes, A. B. *Angew. Chem., Int. Ed.* **1998**, *37*, 402–428.
- (4) Halls, J. J. M.; Baigent, D. R.; Cacialli, F.; Greenham, N. C.; Friend, R. H.; Moratti, S. C.; Holmes, A. B. *Thin Solid Films* **1996**, *276*, 13–20.
- (5) Fisher, T. A.; Lidzey, D. G.; Pate, M. A.; Weaver, M. S.; Whittaker, D. M.; Skolnick, M. S.; Bradley, D. D. C. *Appl. Phys. Lett.* **1995**, *67*, 1355–1357.
- (6) Braun, D.; Heeger, A. J. *Appl. Phys. Lett.* **1991**, *58*, 1982–1984.
- (7) Skotheim, T. A.; Reynolds, J. *Conjugated Polymers: Processing and Applications*, 3rd ed.; Taylor and Francis Group: New York, 2007.
- (8) Skotheim, T. A.; Reynolds, J. *Conjugated Polymers: Theory, Synthesis, Properties, and Characterization*, 3rd ed.; Taylor and Francis Group: New York, 2007.
- (9) Burroughes, J. H.; Bradley, D. D. C.; Brown, A. R.; Marks, R. N.; Mackay, K.; Friend, R. H.; Burns, P. L.; Holmes, A. B. *Nature* **1990**, *347*, 539–541.
- (10) Friend, R. H. *Pure Appl. Chem.* **2001**, *73*, 425–430.
- (11) Hoeben, F. J. M.; Jonkheijm, P.; Meijer, E. W.; Schenning, A. P. H. J. *Chem. Rev.* **2005**, *105*, 1491–1546.
- (12) Schwartz, B. J. *Annu. Rev. Phys. Chem.* **2003**, *54*, 141–172.
- (13) Crone, B. K.; Campbell, I. H.; Davids, P. S.; Smith, D. L. *Appl. Phys. Lett.* **1998**, *73*, 3162–3164.
- (14) Pinner, D. J.; Friend, R. H.; Tessler, N. J. *Appl. Phys.* **1999**, *86*, 5116–5130.
- (15) Chung-Chin, H.; An-En, H.; Show-An, C. *Adv. Mater.* **2008**, *20*, 1982–1988.
- (16) Peng, Z.; Galvin, M. E. *Chem. Mater.* **1998**, *10*, 1785–1788.
- (17) Sheats, J. R.; Chang, Y.-L.; Roitman, D. B.; Stocking, A. *Acc. Chem. Res.* **1999**, *32*, 193–200.
- (18) Sheats, J. R.; Antoniadis, H.; Hueschen, M.; Leonard, W.; Miller, J.; Ron, M.; Roitman, D.; Stocking, A. *Science* **1996**, *273*, 884–888.
- (19) Joachim, L.; Xiaoniu, Y.; Marc, M. K.; Jörgen, S.; Herman, F. M. S.; Sjoerd, C. V.; Werner, G.; Gerald, K.; Ferdinand, H. J. *Appl. Polym. Sci.* **2005**, *97*, 1001–1007.
- (20) Liu, Y.; Yu, G.; Li, Q.; Zhu, D. *Synth. Met.* **2001**, *122*, 401–408.
- (21) Samuel, I. D. W.; Rumbles, G.; Collison, C. *Phys. Rev. B* **1995**, *52*, R11573.
- (22) Ko, S. W.; Jung, B.-J.; Ahn, T.; Shim, H.-K. *Macromolecules* **2002**, *35*, 6217–6223.
- (23) Samuel, I. D. W.; Rumbles, G.; Collison, C. J.; Friend, R. H.; Moratti, S. C.; Holmes, A. B. *Synth. Met.* **1997**, *84*, 497–500.
- (24) Greenham, N. C.; M., S. C.; Bradley, D. D. C.; Friend, R. H.; A.B.; Holmes, A. B. *Nature* **1993**, *365*, 628–630.
- (25) Moratti, S. C.; Cervini, R.; Holmes, A. B.; Baigent, D. R.; Friend, R. H.; Greenham, N. C.; Grüner, J.; Hamer, P. J. *Synth. Met.* **1995**, *71*, 2117–2120.
- (26) Zou, Y.; Hou, J.; Yang, C.; Li, Y. *Macromolecules* **2006**, *39*, 8889–8891.
- (27) Pinto, M. R.; Hu, B.; Karasz, F. E.; Akcelrud, L. *Polymer* **2000**, *41*, 8095–8102.
- (28) Shim, H. K.; Yoon, C. B.; Ahn, T.; Hwang, D. H.; Zyung, T. *Synth. Met.* **1999**, *101*, 134–135.
- (29) Detert, H.; Sugiono, E. *Synth. Met.* **2001**, *122*, 15–17.
- (30) Zhang, C.; Sun, J.; Li, R.; Black, S.; Sun, S. S. *Synth. Met.* **2009**, *160*, 16–21.
- (31) Boardman, F. H.; Grice, A. W.; Rüther, M. G.; Sheldon, T. J.; Bradley, D. D. C.; Burn, P. L. *Macromolecules* **1999**, *32*, 111–117.
- (32) Bates, C. G.; Gujadhur, R. K.; Venkataraman, D. *Org. Lett.* **2002**, *4*, 2803–2806.
- (33) Hui, Z.; Weigu, C.; Dawei, M. *Synth. Commun.* **2007**, *37*, 25–35.
- (34) Kwong, F. Y.; Buchwald, S. L. *Org. Lett.* **2002**, *4*, 3517–3520.
- (35) Gao, P.; Feng, X.; Yang, X.; Enkelmann, V.; Baumgarten, M.; Müllen, K. *J. Org. Chem.* **2008**, *73*, 9207–9213.
- (36) Kobayashi, T.; Hasegawa, Y., Preparation of 1,5- and 1,7-dithia-s-indacene derivatives for use as liquid crystal compounds. U.S. Patent 2005/ 0258398 A1, 11/24/2005.
- (37) Gilman, H.; Martin, G. A. J. *Am. Chem. Soc.* **1952**, *74*, 5317–5319.
- (38) Stille, J. K. *Angew. Chem., Int. Ed.* **1986**, *25*, 508–524.
- (39) Huang, J.; Miller, P. F.; Wilson, J. S.; de Mello, A. J.; de Mello, J. C.; Bradley, D. D. C. *Adv. Funct. Mater.* **2005**, *15*, 290–296.
- (40) Nardes, A. M.; Kemerink, M.; de Kok, M. M.; Vinken, E.; Maturova, K.; Janssen, R. A. *Org. Electron.* **2008**, *9*, 727–734.
- (41) Shaw, M.; Fairchild, M. *Color Res. Appl.* **2002**, *27*, 316–329.
- (42) Mortimer, R. J.; Varley, T. S. *Displays* **2011**, *32*, 35–44.
- (43) Huang, J.; Xu, Z.; Yang, Y. *Adv. Funct. Mater.* **2007**, *17*, 1966–1973.
- (44) Fang-Chung, C.; Jyh-Lih, W.; Sidney, S. Y.; Kuo-Huang, H.; Wen-Chang, C. *J. Appl. Phys.* **2008**, *103*, 103721.
- (45) A Guide to Recording Fluorescence Quantum Yields <http://www.jobinyvon.com/usadivisions/fluorescence/applications/quantumyieldstrad.pdf> (accessed March 22, 2012).